

BCSJ Award Article

Highly Efficient Method for Constructing a Single-Stranded Comb-Like Oligonucleotide via Reversible Photocrosslinking

Shinzi Ogasawara,[1] Yoshinaga Yoshimura,[1] Masayuki Hayashi,[2] Isao Saito,[3] and Kenzo Fujimoto*[1]

[1]School of Materials Science, Japan Advanced Institute of Science and Technology, 1-1 Asahidai, Nomi 923-1292

[2]Department of Synthetic Chemistry and Biological Chemistry, Kyoto University, Kyoto 606-8501

[3]School of Engineering, NEWCAT Institute, Nihon University, Tamura, Koriyama 963-8642

Received March 13, 2007; E-mail: kenzo@jaist.ac.jp

Branched oligodeoxyribonucleotides (ODNs) are key molecules in constructing nano-scale structures such as DNA lattices, dendrimer-like DNA as well as DNA devices including DNA walkers, DNA memory, and DNA computer. In this paper, two types of highly efficient methods were used to construct the comb-like DNA by using template-directed reversible DNA photocrosslinking via 5-(2-carbamoylvinyl)-2′-deoxyuridine (^{cv}U). The efficiency and thermodynamic stability of three types of reversible DNA photocrosslinked, linear ODN, single-branched ODN (5′-end) and single-branched ODN (mid) reported previously, were also compared. The results show that the most efficient one of the three is a single-branched ODN (5′-end), despite its low thermodynamic stability. In addition, we also showed that this reversible photocrosslinking method is applicable to nanotechnology by constructing comb-like DNA. This method should have great potential in nanotechnology by serving as a platform for fabrication and synthesis, because their sizes and structures can be changed through the alteration of building blocks. We believe that this method is versatile and may find a myriad of applications in the nano-biotechnology field.

Because of the experiments of Seeman et al.,[1] the potential of using DNA as a construction material for synthetic nanometer-scale objects has been recognized within bioorganic chemistry. In particular, branched ODNs have become key molecules for constructing nano-scale architectures and devices. Branched DNA molecules have various uses in signal amplification technology[2] and in several types of nanotechnology such as DNA computing,[3] DNA nano architectures,[4] DNA sensors,[5] and nanoelectronic devices.[6] DNA lattices[7] and dendrimer-like DNA[8] have been constructed from a rich set of branched DNA. Various autonomous DNA walker devices based on DNA cleavage and ligation of branched DNA using various enzymes have also been explored.[9]

There are two types of branched DNA, topologically double-stranded branched DNA complexes assembled from linear DNA polymers (branch junction motifs),[10] as reported by Seeman et al., and covalently single-stranded branched DNA polymers.[11] The strucutre of the covalently branched DNA is resistant to high temperature. In contrast, the thermal stability of the topologically branched DNA is relatively low because of self-assembly of programmed sequences according to Watson–Crick complementarity. Most covalently branched DNA has been chemically on solid supports using phosphoramidites containing a branched structural unit. Such branched DNA has several practical disadvantages such as the limited symmetry of the branched sequences and structural restriction. These methods cannot be used to create single-stranded comb-like DNA, although the dendrimer-like DNA has been readily synthesized. There is a universal need to find a new method to synthesize couple covalently and asymmetrically sequenced branched coupled DNA that can be widely used as a platform for building DNA nanodevices and architectures.

Here, we report highly efficient methods for constructing comb-like DNA by using template-directed[12] reversible DNA photocrosslinking via 5-(2-carbamoylvinyl)-2′-deoxyuridine (^{cv}U). We have been studying artificial DNA bases, for example ^{cv}U shown in Fig. 1, as a tool for photochemical DNA manipulation[13] and succeeded in not only the synthesis of complex DNA structures, such as branched DNA, end-capped DNA, and padlocked plasmid DNA,[14] but also mutant

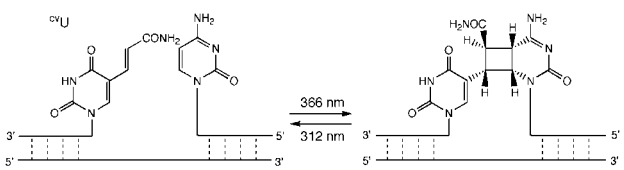

Fig. 1. Template-directed reversible DNA photocrosslinking via ^{cv}U. Irradiation at 366 nm caused the formation of a cyclobutane ring between the vinyl group of ^{cv}U and the pyrimidine ring at 3′-end in DNA. Conversely, photoirradiation at 312 nm cleaved the cyclobutane ring.

Published on the web November 13, 2007; doi:10.1246/bcsj.80.2124

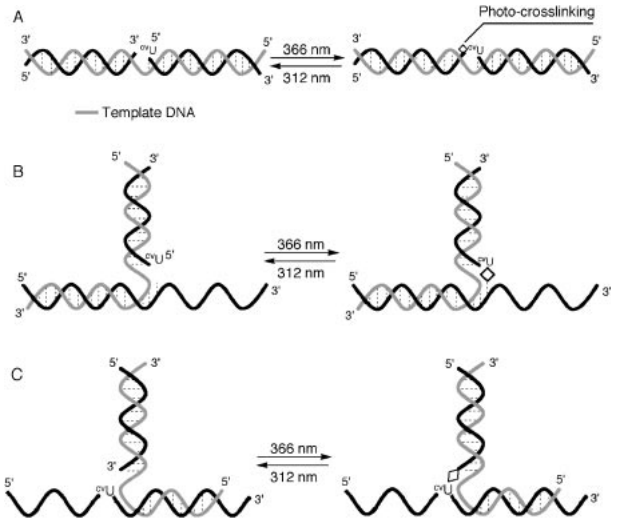

Fig. 2. Schematic illustration of three typical reversible DNA photocrosslinking for the construction of DNA nano-structures. (A) Construction of linear ODN (L-ODN), (B) Single-branched ODN [SB-ODN (5′-end)], ^{cv}U was contained at the 5′-end in branch ODN and (C) Single-branched DNA [SB-ODN (mid)], ^{cv}U was contained at the midstream in base ODN.

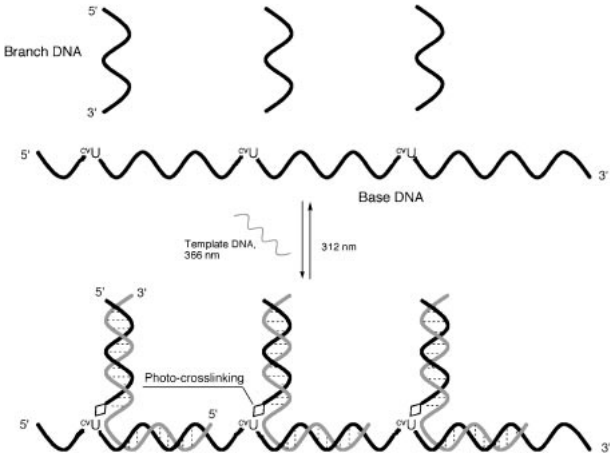

Fig. 3. Idealized drawing for the construction of a comb-like single-stranded oligonucleotide based on the template-directed reversible photocrosslinking. Base-DNA and branch-DNA were photoligated by irradiating at 366 nm in the presence of a template. Irradiation at 312 nm caused the ligated product to revert to the original DNA.

Table 1. Oligodeoxynucleotides (ODNs) Used in This Study

	Sequences (5′–3′)
ODN **1a**	^{cv}UGCGTCAG
ODN **1b**	CGAGTCGT
ODN **1c**	CTGACGCAACGACTCG
ODN **2b**	CGAGTCGTGAAAAA
ODN **3a**	AAAAAG^{cv}UGCGTCAG
ODN **3b**	CGAGTCGT
ODN **4a**	^{cv}UGACAG
ODN **4b**	^{cv}UGCGTG
ODN **4c**	AAAGGACGC(A)$_{17}$ACTGTGCAAAAAA
ODN **4d**	CTCACAGCGTCC
ODN **4e**	CACGCAGCACAG
ODN **5a**	AAAG^{cv}UGCGTGAAAG^{cv}UGCGTG
ODN **5b**	CAGTGT
ODN **5c**	CACGCAACACTG

detection.[15] Recently, we have developed a method that can directly process DNA similar to RNA processing and another method to synthesize R-shaped DNA as a unique structure of lariat DNA.[14a] Photochemical ligation can be performed effectively even in an extremely tight space unlike enzymatic ligation, without crucial conformation change.[16]

Three typical reversible DNA photocrosslinks via ^{cv}U are shown in Fig. 2. The first one is a linear ODN (L-ODN); an ODN containing ^{cv}U at the 5′-end and one containing a pyrimidine ring at the 3′-end are irradiated at 366 nm in the presence of a template, producing a linear combination between the two ODNs. Second is a single-branched ODN (5′-end) [SB-ODN (5′-end)]; SB-ODN (5′-end) can also be synthesized in a similar way to L-ODN, i.e. an ODN containing ^{cv}U at the 5′-end and an ODN containing a pyrimidine ring at internal residue are irradiated at 366 nm in the presence of a template, producing a branched combination between the two ODNs. The last one is a single-branched ODN (mid) [SB-ODN (mid)]; this type has recently been examined as a more useful and highly efficient method to synthesize branched ODN, based on template-directed DNA photocrosslinking in which ^{cv}U is contained in the midstream of the ODN. In this paper, these three types of photocrosslinks were compared based on aspects of efficiency and thermodynamic stability. Moreover, the feasibility of the reversible photocrosslinking method for constructing comb-like DNA (shown in Fig. 3) was demonstrated through the synthesis of single-stranded double-branched ODN (DB-ODN) using the two means of constructing SB-ODN as described above.

Results and Discussion

Construction of Three Typical Structures by Reversible DNA Photocrosslinking. The ODNs used in this study are summarized in Table 1. ^{cv}U-containing ODNs were synthesized using standard phosphoramidite chemistry on a DNA synthesizer using nucleoside phosphoramidite of ^{cv}U. Following deprotection and oligomer purification, ODNs containing ^{cv}U were characterized by analyzing the nucleoside composition and MALDI-TOF MS. To obtain the formation efficiency of L-ODN, SB-ODN (5′-end), and SB-ODN (mid), we initially constructed these structures individually. When ODNs (ODN **1a** + ODN **1b**/ODN **1c** for L-ODN, ODN **1a** + ODN **2b**/ODN **1c** for SB-ODN (5′-end), and ODN **3a** + ODN **3b**/ODN **1c** for SB-ODN (mid)) were irradiated at 366 nm for 3 h on ice, we observed the rapid appearance of the peak for L-ODN, SB-ODN (5′-end), and SB-ODN (mid), in 96%, 94%, and 96% yields, respectively, as determined by capillary gel electrophoresis (CGE), and the concomitant disappearance of the starting ODNs except the template ODN (Fig. 4). These photoproducts were purified by HPLC and identified by MALDI-TOF MS, indicating that the photoproducts were L-ODN, SB-ODN (5′-end), and SB-ODN (mid). Enzymatic

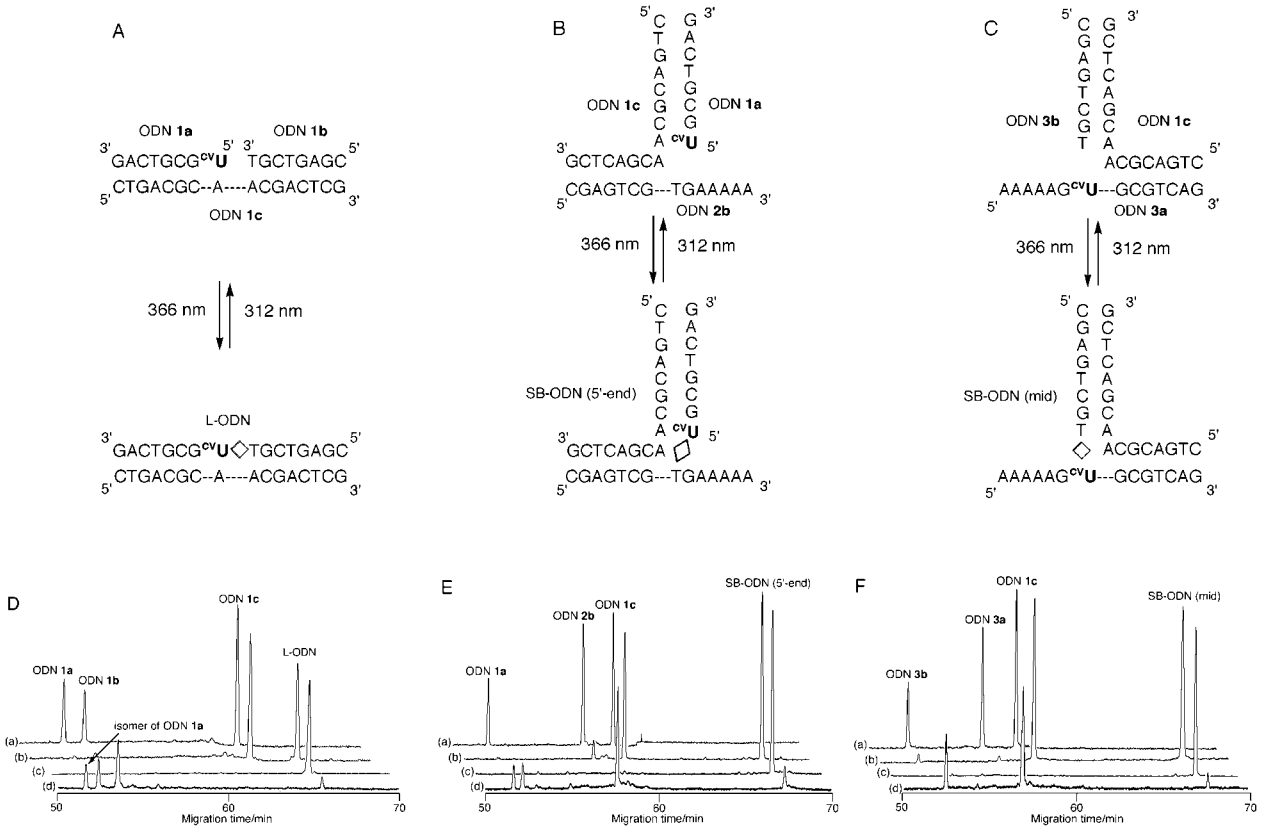

Fig. 4. Schemes and CGE analysis for each types of template-directed reversible photocrosslinking (A) of L-ODN, (B) of SB-ODN (5′-end) and (C) of SB-ODN (mid). (D) CGE analysis for reversible construction of the L-ODN, a) ODN **1a** + ODN **1b**/ODN **1c**, before photoirradiation; b) Irradiation to reaction mixture at 366 nm for 1 h (96% yield); c) Purification of the L-ODN after 366 nm irradiation; d) Irradiation to purified L-ODN at 312 nm for 15 min (94% conv.). (E) CGE analysis for reversible construction of the SB-ODN (5′-end), a) ODN **1a** + ODN **2b**/ODN **1c**, before photoirradiation; b) Irradiation to reaction mixture at 366 nm for 1 h (96% yield); c) Purification of the SB-ODN (5′-end) after 366 nm irradiation; d) Irradiation to purified SB-ODN (5′-end) at 312 nm for 15 min (91% conv.). (F) CGE analysis for reversible construction of the SB-ODN (mid), a) ODN **3a** + ODN **3b**/ODN **1c**, before photoirradiation; b) Irradiation of the reaction mixture at 366 nm for 3 h (95% yield); c) Purification of the SB-ODN (mid) after 366 nm irradiation; d) Irradiation of the purified L-ODN at 312 nm for 15 min (94% conv.).

digestion of each isolated photoproducts followed by HPLC analysis indicated the formation of dA, dC, dG, and dT in a ratio of 2:4:6:2 (L-ODN), 7:4:4:2 (SB-ODN (5′-end)), and 7:4:4:2 (SB-ODN (5′-end)) together with a new product (Data not shown). Irradiation of the purified photocrosslinked products at 312 nm for 15 min caused the rapid disappearance of the photoproducts and formation of the original ODNs. CGE analysis of the 312 nm irradiated mixture confirmed the clean formation of ODN **1a** + ODN **1b**, ODN **1a** + ODN **2b**, and ODN **3a** + ODN **3b** from L-ODN, SB-ODN (5′-end), and SB-ODN (mid), respectively, as shown by the migration time (Fig. 4). Analysis by MALDI-TOF MS of the newly formed ODNs also indicated that these ODNs were ODN **1a** + ODN **1b** for L-ODN, ODN **1a** + ODN **2b** for SB-ODN (5′-end), and ODN **3a** + ODN **3b** for SB-ODN (mid). Figure 5 shows a comparison of photo-reactivity with L-ODN versus SB-ODN (5′-end) versus SB-ODN (mid). For each photoreaction, highly efficient photocrosslinking was clearly observed upon irradiation at 366 nm for 3 h, and photo-splitting was observed upon irradiation at 312 nm for 15 min with >90% conversion. The formation of SB-ODN (mid) was nearly two times slower than that of SB-ODN (5′-end) at the beginning. Interestingly, the branched crosslinking of SB-ODN (5′-end) was faster than L-ODN. Conversely, the photo-splitting of SB-ODN (mid) was the fastest, and SB-ODN (5′-end) was the slowest. The difference in reactivity is attributed mainly to the positional relation between ^{cv}U and T. In fact, an appropriate distance and a parallel arrangement between the vinyl group in ^{cv}U and T are needed to obtain the high reactivity.

Thermodynamic Experiments. To examine the thermodynamic properties of complexes, the melting temperature of various concentrations of the complexes containing native duplex, L-ODN, SB-ODN (5′-end), and SB-ODN (mid) were measured to prepare van't Hoff plots. The thermodynamic parameters of these complexes are summarized in Table 2. For both SB-ODNs, i.e., SB-ODN (5′-end) and SB-ODN (mid), the T_m values decreased by 14.4–15.0 °C as compared to those of the native duplex (between ODN **1c** and complementary strand, 5′-d(CGAGTCGTTGCGTCAG)-3′), where as the T_m values of L-ODN decreased by 11.6 °C as compared to those of the native duplex. The differences in the enthalpy and entropy changes between the native duplex and L-ODN were 11.2 kJ mol^{-1} and 30.7 J mol^{-1} K^{-1}, respectively. In contrast, the differences in the enthalpy and entropy changes

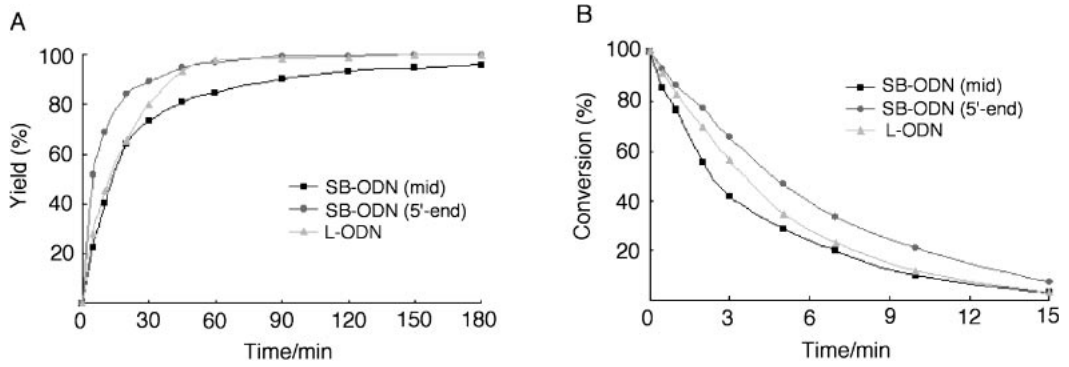

Fig. 5. Time course of (A) photocrosslinking and (B) photo-splitting of L-ODN (▲), SB-ODN (5′end) (●), and SB-ODN (mid) (■) as followed by CGE analysis.

Table 2. Thermodynamic Parameters for Duplex Formation[a)]

	T_m/°C	ΔT_m/°C	$\Delta H°$/kJ mol^{-1}	$\Delta\Delta H°$/kJ mol^{-1}	$\Delta S°$/J mol^{-1} K^{-1}	$\Delta\Delta S°$/J mol^{-1} K^{-1}	$\Delta G°_{298K}$/kJ mol^{-1}
Native[b)]	63.2	—	−37.4	—	−105	—	−6.17
L-ODN	51.6	−11.6	−26.2	+11.2	−74.3	+30.7	−4.05
SB-ODN (5′-end)	48.8	−14.4	−23.8	+13.6	−67.4	+37.6	−3.74
SB-ODN (mid)	48.2	−15.0	−24.3	+13.1	−69.0	+36.0	−3.71

a) Determined in 50 mM dimethylarsinate and 100 mM NaCl, pH 7.0. A ramp rate of 0.5 °C min^{-1} with hold time of 5 min was used over the temperature range of 20 to 80 °C to record the DNA melting curve. b) Native stands for a duplex between ODN **1c** and complementary strand, 5′-d(CGAGTCGTTGCGTCAG)-3′.

between the native duplex and both SB-ODNs were 13.1–13.6 kJ mol^{-1} and 36.0–37.6 J mol^{-1} K^{-1}, respectively. In the cases of the complexes of both SB-ODNs, the T_m values of the SB-ODNs complexes had large differences in both enthalpy and entropy changes from those of the native or L-ODN duplexes, indicating that the duplex between SB-ODN and ODN **3a** causes a larger deformation than the L-ODN duplex. The changes in the enthalpy terms may be attributed to the significant decrease in the hydrogen bondings around the position where the photocrosslinking occurred. In addition, the changes in the entropy term may be attributed to the disordered structure of the duplex around the photocrosslinking position. The decrease in the thermodynamic properties for SB-ODN is due to fluctuation of the extra branch. From this point, the base ODN (ODN **2b** and ODN **3a**) is probably bent at the photocrosslinking point rather than the template ODN **1c** being bent, shown in Figs. 4B and 4C.

Construction of DB-ODN by Two Strategies. Finally, to demonstrate the usability of photocrosslinking for the construction of a DNA nano-structure, we examined the effects of the construction of double-branched ODN (DB-ODN), using the two strategies used in the synthesis of SB-ODN (Fig. 6). Figure 7 presents an autoradiogram of a denaturing polyacrylamide gel electrophoresis for the photoreaction of strategy 1. Polyacrylamide gel electrophoresis was chosen for following the photocrosslinking process instead of CGE because of using the relatively long base stand. When ODNs **4a**–**4c** were irradiated at 366 nm for 1 h in the presence of templates ODN **4d** and **4e**, the expected 51-mer DB-ODN (5′-end) was produced (Lane 2), and the resulting photoproduct quantitatively reverted to the original ODNs upon at 312 nm irradiation (Lane 3). On the other hand, when ODN **4c** was irradiated

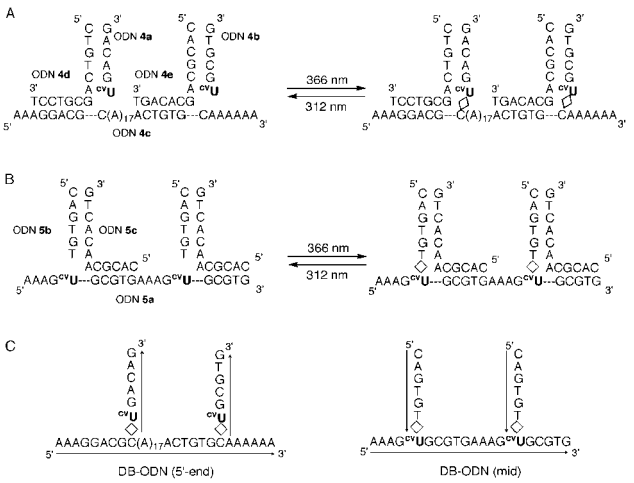

Fig. 6. Schematic drawing for (A) Strategy 1 in which DB-ODN (5′-end) was made from two branch ODNs, ODN **4a** and ODN **4b**, containing ^{cv}U at 5′-end, and (B) Strategy 2 in which DB-ODN (mid) was made from base ODN **5a** containing two ^{cv}U at midstream (C) Structure for two types of single-stranded DB-ODN produced by Strategy 1 and Strategy 2. Tail of both branches in DB-ODN (5′-end) are 3′-end, while that are 5′-end in DB-ODN (mid).

at 366 nm without either of the branch components (Lane 4; without ODN **4a** and ODN **4d**, Lane 6; without ODN **4b** and ODN **4e**, Lane 8; without ODN **4d**, Lane 9; without ODN **4e**), SB-ODN (5′-end) formed. Figure 8 shows a CGE profile of the photoirradiated mixture of ODN **5a** and ODN **5b** in the presence or absence of template ODN **5c** (Strategy 2). It shows the clean and efficient formation of the expected 32-mer DB-

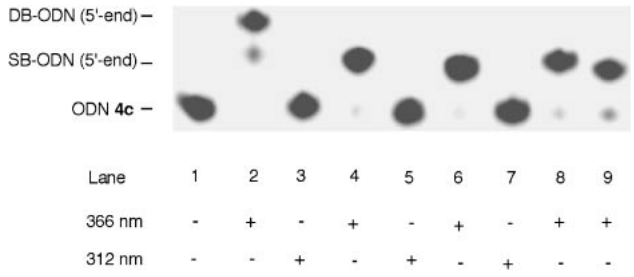

Fig. 7. Autoradiogram of a denaturing polyacrylamide gel electrophoresis of the photoreaction of ODN **4a**, ODN **4b**, and ^{32}P-5′-end-labeled ODN **4c** in the presence or absence of template ODN **4d** or ODN **4e** on ice. Lane 1, ODN **4a** + ODN **4b** + ODN **4c**/ODN **4d** + ODN **4e**, before photoirradiation; lane 2, irradiation of lane 1 at 366 nm for 1 h (quant); lane 3, irradiation of lane 2 at 312 nm for 0.5 h (quant); lane 4, ODN **4b** + ODN **4c**/ODN **4e**, irradiation at 366 nm for 1 h (95%); lane 5, irradiation of lane 4 at 312 nm for 0.5 h (quant); lane 6, ODN **4a** + ODN **4c**/ODN **4d**, irradiation at 366 nm for 1 h (95%); lane 7, irradiation of lane 6 at 312 nm for 0.5 h (quant); lane 8, ODN **4a** + ODN **4b** + ODN **4c**/ODN **4e**, irradiation at 366 nm for 1 h (95%); lane 9, ODN **4a** + ODN **4b** + ODN **4c**/ODN **4d**, irradiation at 366 nm for 1 h (88%).

ODN (mid) and the complete disappearance of ODN **5a** and ODN **5b** (Fig. 8A); however, no photoproduct was observed in the absence of template ODN **5c** (Fig. 8B). The isolated new product was characterized by MALDI-TOF MS and enzymatic digestion. Irradiation of DB-DNA (mid) at 312 nm resulted in complete reversion to ODN **5a** and ODN **5b**, as determined by MALDI-TOF MS (Fig. 8C). DB-ODN (mid) was synthesized and reverted to the original ODNs through the SB-ODN (mid) at the upstream ^{cv}U or downstream ^{cv}U. We observed these peaks clearly at the beginning of the irradiation at 366 or 312 nm around 80 min at Figs. 8A and 8C.

Conclusion

In the three typical reversible DNA photocrosslinking via ^{cv}U, there was a difference in the reaction rate during irradiation at 366 or 312 nm, although highly efficient photocrosslinking and photo-splitting were clearly observed by irradiation at 366 nm for 3 h and 312 nm for 15 min, respectively. The amount of SB-ODN (mid) was nearly half that of SB-ODN (5′-end) at the beginning. We also demonstrated the feasibility of the reversible photocrosslinking method for constructing DNA nano-structure, as evidenced by the synthesis of single-stranded DB-ODN using two strategies. Both strategies efficiently afforded DB-ODN upon irradiation at 366 nm without any side reaction, and cleavage upon irradiation at 312 nm. This demonstration indicates that we can conceptually construct single-stranded comb-formed DNA from a long base-DNA and some branch DNA, which could not be created by previous methods. Future studies will involve the synthesis of more than 100-mer base DNA by introducing ^{cv}U via an enzymatic PCR method. These methods are well suited to prepare DNA nanodevices such as the DNA walker, DNA computer, and DNA memory as well as nano architectures such as two- and three-dimensional DNA structures. We believe

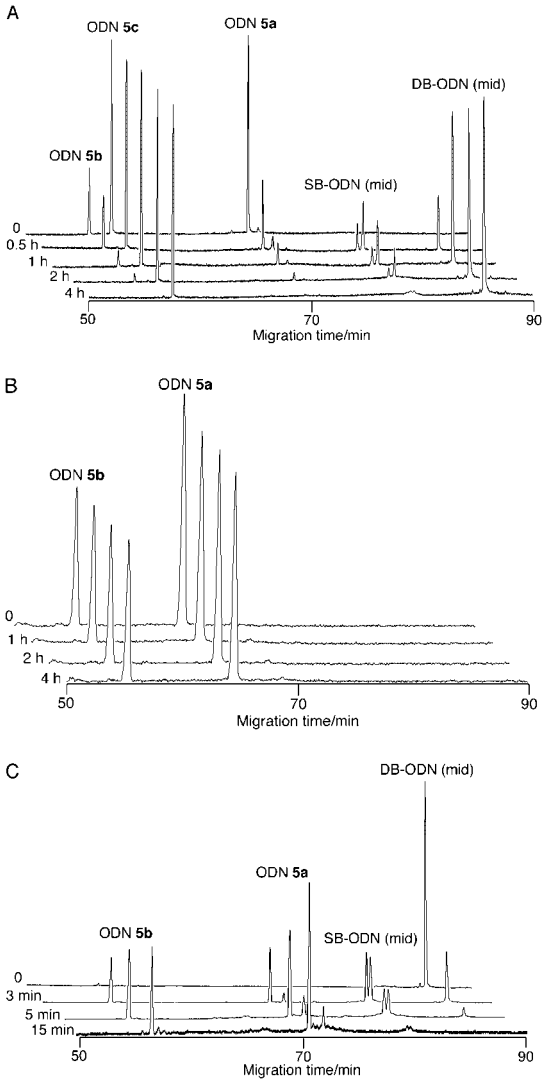

Fig. 8. CGE analysis for reversible photocrosslinking of DB-ODN (mid). DB-ODN (mid) was synthesized through the SB-ODN (mid) at the upstream ^{cv}U or downstream ^{cv}U. These peaks were clearly observed at the beginning of the irradiation with 366 nm and 312 nm. (A) Construction of DB-ODN (mid) by irradiation at 366 nm for 4 h; >99% yield, reaction mixture containing ODN **5a** + ODN **5b**/ODN **5c** (B) Irradiation at 366 nm in the absence of template ODN **5c**, No SB-ODN (mid) and DB-ODN (mid) was observed. (B) Irradiated at 366 nm for 4 h; >99% yield (C) Photo-splitting of purified DB-ODN by irradiation at 312 nm for 15 min; >99% conversion.

that this method is versatile, and there should be a myriad of applications for it in the nano-biotechnology field.

Experimental

Materials. 2-Cyanoethoxybis(diisopropylamino)phosphine was purchased from Aldrich. The reagents for the DNA synthesizer such as I_2 solution (I_2/H_2O/pyridine/tetrahydrofuran, 3:2:19:76) A-, G-, C-, and T-β-cyanoethylphosphoramidites, 1*H*-tetrazole, acetonitrile, and CPG support were purchased from Glen Research. Artificial ODNs were synthesized on an Applied Biosystems 3400 DNA/RNA synthesizer. Native ODNs were

purchased form Hokkaido System Science. Calf intestine alkaline phosphatase (AP) was purchased from Promega. Nuclease P1 was purchased from Yamasa. Irradiation was performed by using Funakoshi transilluminator (TFL-40, 366 nm, 25 W) or Funakoshi transilluminator (TR-312R/J, 312 nm, 25 W).

Oligonucleotide Synthesis and Characterization. ^{cv}U was synthesized from 5-iodo-2′-deoxyuridine using a previously reported procedure.[11c] ^{cv}U-containing ODNs were prepared by using the β-cyanoethylphosphoramidite method on controlled pore glass supports using an Applied Biosystems, 3400 DNA synthesizer and the standard method. After automated synthesis, the oligomers were deprotected by treating with concentrated aqueous ammonia at 65 °C for 5 h and purified by HPLC on a Nacalai Tesque, COSMOSIL 5C^{18}-AR-2 (10.0 × 250 mm^2). The eluent was 0.05 M ammonium formate containing 5–12% acetonitrile, and the elution was performed with a linear gradient of 30 min and a flow rate of 3.0 mL min^{-1}. ODNs containing modified nucleotides were fully digested with calf intestine alkaline phosphatase (50 U mL^{-1}), snake venom phosphodiesterase (0.15 U mL^{-1}) and P1 nuclease (50 U mL^{-1}) at 37 °C for 4 h. The digested solutions were analyzed by HPLC on a Nacalai Tesque, COSMOSIL 5C^{18}-AR-2 (4.6 × 150 mm). the eluent was 0.05 M ammonium formate containing 3–20% acetonitrile, and elution was performed with a linear gradient of 30 min and a flow rate of 1.0 mL min^{-1}. The concentration of each ODNs were determined by comparing the peak areas with the standard solution containing dI, dC, dG, and dT at a concentration of 0.1 mM. The molecular mass of the ODNs was determined by MALDI-TOF MS. 5′-d(^{cv}UGCGTCAG)-3′ (ODN **1a**) Calcd. for [M + H]$^+$: 2480.45, Found: 2480.46, 5′-d(AAAAAG^{cv}UGCGTCAG)-3′ (ODN **3a**) Calcd. for [M + H]$^+$: 4376.94, Found: 4376.99, 5′-d(AAAG^{cv}UGCGTGAAAG^{cv}UGCGTG)-3′ (ODN **5a**) Calcd. for [M + H]$^+$: 6357.20, Found: 6358.09, 5′-d(CGAGTCGT)-3′ (ODN **1b**) Calcd. for [M + H]$^+$: 2425.62, Found: 2425.62, 5′-d(CGAGTCGTGAAAAA)-3′ (ODN **2b**) Calcd. for [M + H]$^+$: 4320.88, Found: 4320.88, 5′-d(CAGTGT)-3′ (ODN **5b**) Calcd. for [M + H]$^+$: 1805.34, Found: 1805.07, 5′-d(CTGACGCAACGACGACTCG)-3′ (ODN **1c**) Calcd. for [M + H]$^+$: 4851.22, Found: 4851.22, 5′-d(CACGCAACACTG)-3′ (ODN **5c**) Calcd. for [M + H]$^+$: 3598.67, Found: 3598.71.

Preparation of ^{32}P-5′-End-Labeled ODN. ODN **4c** (400 pmol, strand concentration) was 5′-end-labeled by phosphorylation with 4 μL of [γ-^{32}P] ATP and 4 μL of T4 polynucleotide kinase using standard procedures. The 5′-end-labeled ODNs were recovered by precipitating with ethanol and further purified by 15% denaturing gel electrophoresis and isolated by the crush and method.

Photoreaction of L-ODN. A reaction mixture containing 5′-d(^{cv}UGCGTCAG)-3′ (ODN **1a**), 5′-d(CGAGTCGT)-3′ (ODN **1b**) (each 20 μM), and 5′-d(CTGACGCAACGACTCG)-3′ (ODN **1c**) (25 μM) in 50 mM sodium dimethylarsinate buffer (pH 7.0) and 100 mM NaCl was irradiated with a transilluminator at 366 nm at 0 °C for 3 h. Purification was performed on a Nacalai Tesque, COSMOSIL 5C^{18}-AR-2 (4.6 × 150 mm^2). The eluent was 0.05 M ammonium formate containing 5–10% acetonitrile, and the elution was performed with a linear gradient of 30 min and a flow rate of 1.0 mL min^{-1}, at 50 °C. The purified L-ODN were determined by MALDI-TOF MS. Calcd. for [M + H]$^+$: 4907.32, Found: 4907.31. A solution containing isolated photoligated L-ODN in a quartz capillary cell was irradiated at room temperature with a transilluminator at 312 nm for 15 min. After irradiation, the aliquot was collected and subjected to CGE analysis.

Photoreaction of SB-ODN (5′-end). A solution containing 5′-d(^{cv}UGCGTCAG)-3′ (ODN **1a**), 5′-d(CGAGTCGTGAAAAA)-3′ (ODN **2b**) (each 20 μM), and 5′-d(CTGACGCAACGACTCG)-3′ (ODN **1c**) (25 μM) in 50 mM sodium dimethylarsinate buffer (pH 7.0) and 100 mM NaCl was irradiated at 366 nm at 0 °C for 3 h. SB-ODN (5′-end) was purified on a Nacalai Tesque COSMOSIL 5C^{18}-AR-2 (4.6 × 150 mm^2) and its molecular mass was determined by MALDI-TOF MS. Calcd. for [M + H]$^+$: 6802.58, Found 6802.61. A solution containing isolated photoligated SB-ODN (5′-end) in a quartz capillary cell was irradiated at room temperature with a transilluminator at 312 nm for 15 min.

Photoreaction of SB-ODN (mid). A solution containing 5′-d(AAAAAG^{cv}UGCGTCAG)-3′ (ODN **3a**), 5′-d(CGAGTCGT)-3′ (ODN **3b**) (each 20 μM), and 5′-d(CTGACGCAACGACTCG)-3′ (ODN **1c**) (25 μM) in 50 mM sodium dimethylarsinate buffer (pH 7.0) and 100 mM NaCl was irradiated at 366 nm at 0 °C for 3 h. SB-ODN (mid) was purified on a Nacalai Tesque COSMOSIL 5C^{18}-AR-2 (4.6 × 150 mm^2) and its molecular mass was determined by MALDI-TOF MS. Calcd. for [M + H]$^+$: 6802.58, Found: 6802.59. A solution containing isolated photoligated SB-ODN (mid) in a quartz capillary cell was irradiated at room temperature with a transilluminator at 312 nm for 15 min. After irradiation, the aliquot was collected and subjected to CGE analysis and MALDI-TOF MS. 5′-d(CGAGTCGT)-3′ (ODN **3b**) Calcd. for [M + H]$^+$: 2425.62, Found: 2425.45.

Photoreaction of DB-ODN (5′-end). A reaction mixture containing ^{32}P-5′-end-labeled 5′-d(AAAGGACGC(A)$_{17}$ACTGTGCAAAAAA)-3′ (ODN **4c**), 5′-d(^{cv}UGACAG)-3′ (ODN **4a**), and 5′-d(^{cv}UGCGTG)-3′ (ODN **4b**) (each 20 μM) in the presence or absence of 5′-d(CTCACAGCGTCC)-3′ (ODN **4d**) and 5′-d(CACGCAGCACAG)-3′ (ODN **4b**) (each 25 μM) in 50 mM sodium dimethylarsinate buffer (pH 7.0) in a quartz capillary cell was irradiated at 0 °C with transilluminator (366 nm) under otherwise identical conditions. To the reaction mixture was added 10 μL of loading buffer to quench the reaction and the sample (1–2 μL, ca. 2–4 × 10^3 cpm) was loaded onto 15% polyacrylamide and 7 M urea denaturing gel and electrophoresed at 700 V for 30 min. The gel was dried and exposed to X-ray film with intensifying sheets at −80 °C.

Photoreaction of DB-ODN (mid). A solution containing 5′-d(AAAG^{cv}UGCGTGAAAG^{cv}UGCGTG)-3′ (ODN **5a**) 20 μM, 5′-d(CAGTGT)-3′ (ODN **5b**) 40 μM, and 5′-d(CACGCAACACTG)-3′ (ODN **5c**) 50 μM in 50 mM sodium dimethylarsinate buffer (pH 7.0) and 100 mM NaCl was irradiated at 366 nm at 0 °C for 4 h. Purification was performed on a Nacalai Tesque, COSMOSIL 5C^{18}-AR-2 (4.6 × 150 mm). The eluent was 0.05 M ammonium formate containing 4–12% acetonitrile, and the elution was performed with a linear gradient of 60 min and a flow rate of 1.0 mL min^{-1}, 50 °C. The molecular mass of the purified DB-ODN were determined by MALDI-TOF MS. Calcd. for [M + H]$^+$: 9971.69, Found: 9971.67. A solution containing isolated photoligated DB-ODN in a quartz capillary cell was irradiated at room temperature with a transilluminator at 312 nm for 15 min. After irradiation, the aliquot was collected and subjected to CGE analysis and MALDI-TOF MS. 5′-d(AAAG^{cv}UGCGTGAAAG^{cv}UGCGTG)-3′ (ODN **5a**) Calcd. for [M + H]$^+$: 6357.20, Found: 6358.21, 5′-d(CAGTGT)-3′ (ODN **5b**) Calcd. for [M + H]$^+$: 1805.34, Found: 1805.34.

MALDI-TOF/MS Analysis. MALDI-TOF mass spectra were measured on a Voyager-DE PRO-SF BioSpectrometry™ Workstation from Applied Biosystems (Foster City, USA) with acceleration voltage of 20 kV, in positive mode. Each sample

was analyzed using a 3-hydroxypicolinic acid matrix and the data was calibrated using a two-point internal standard.

Capillary Gel Electrophoresis (CGE) Analysis. The progress of each photoreaction was monitored by capillary gel electrophoresis (CGE) on a Beckman Coulter, P/ACE™ MDQ equipped with UV absorbance detector. Separations were performed at an applied voltage of 20 kV and a temperature of 30 °C and were detected by monitored using their absorbance at 254 nm.

Melting Temperature Measurement. After photoligation, melting temperatures were measured by using a Beckman Coulter DU800 spectrometer. The absorbance of the sample (0.5–3.0 μM strand concentration, 50 mM sodium cacodylate buffer (pH 7.0) and 100 mM NaCl) was monitored at 260 nm from 20 to 80 °C at a heating rate of 0.5 °C per min. The melting temperatures were determined using the derivative method incorporated in the DU 800 application software.

Enzymatic Digestion. After the purification of photoproducts by HPLC, SB-ODN (mid) and DB-ODN were fully digested with calf intestine alkaline phosphatase (50 U mL^{-1}), snake venom phosphodiesterase (0.15 U mL^{-1}) and P1 nuclease (50 U mL^{-1}) at 37 °C for 4 h. The digested solutions were analyzed by using HPLC on a Nacalai Tesque COSMOSIL $5C^{18}$-AR-2 (4.6×150 mm^2). The eluent was 0.05 M ammonium formate containing 3–20% acetonitrile, and the elution was performed with a linear gradient of 30 min and a flow rate of 1.0 mL min^{-1}.

References

Dedicated to Professor Isao Saito on the occasion of his 65th birthday.

1 a) N. C. Seeman, *Biochemistry* **2003**, *42*, 7259. b) S. Liao, N. C. Seeman, *Science* **2004**, *306*, 2072. c) Y. Yan, X. Zhang, Z. Shen, N. C. Seeman, *Nature* **2002**, *415*, 62. d) C. Mao, W. Sun, Z. Shen, N. C. Seeman, *Nature* **1999**, *397*, 144. e) Y. Zhang, N. C. Seeman, *J. Am. Chem. Soc.* **1994**, *116*, 1661.

2 a) M. L. Collins, B. Irvine, D. Tyner, E. Fine, C. Zayati, C. Chang, T. Horn, D. Ahle, J. Detmer, L. P. Shen, J. Kolberg, S. Bushnell, M. S. Urdea, D. D. Ho, *Nucleic Acids Res.* **1997**, *25*, 2979. b) M. S. Urdea, *Biotechnology* **1994**, *12*, 926.

3 a) P. Sa-Ardyen, N. Jonoska, N. C. Seeman, *J. Am. Chem. Soc.* **2004**, *126*, 6648. b) S. Ogasawara, K. Fujimoto, *Chem. Lett.* **2005**, *34*, 378.

4 a) M. Endo, N. C. Seeman, T. Majima, *Angew. Chem.* **2005**, *117*, 6228. b) Y. Ke, Y. Liu, J. Zhang, H. Yan, *J. Am. Chem. Soc.* **2006**, *128*, 4414. c) U. Feldkamp, C. M. Niemeyer, *Angew. Chem., Int. Ed.* **2006**, *45*, 1856. d) R. P. Goodman, I. A. T. Schaap, C. F. Tardin, C. M. Efben, R. M. Berry, C. F. Schmidt, A. J. Turberfield, *Science* **2005**, *310*, 1661. e) W. M. Shih, J. D. Quispe, G. F. Joyce, *Nature* **2004**, *427*, 618. f) D. Mitra, N. D. Cesare, H. F. Sleiman, *Angew. Chem., Int. Ed.* **2004**, *43*, 5804. g) M. Scheffler, A. Dorenbeck, S. Jordan, M. Wustefeld, G. Kiedrowski, *Angew. Chem., Int. Ed.* **1999**, *38*, 3311.

5 F. Nakamura, E. Ito, Y. Sakao, N. Ueno, I. N. Gatuna, F. S. Ohuchi, M. Hara, *Nano Lett.* **2003**, *3*, 1083.

6 H. A. Becerril, R. M. Stoltenberg, D. R. Wheeler, R. C. Davis, J. N. Harb, A. T. Woolley, *J. Am. Chem. Soc.* **2005**, *127*, 2828.

7 a) S. H. Park, R. Barish, H. Li, J. H. Reif, G. Finkelstein, H. Yan, T. H. LaBean, *Nano Lett.* **2005**, *5*, 693. b) H. Yan, S. H. Park, G. Finkelstein, J. H. Reif, T. H. LaBean, *Science* **2003**, *301*, 1882. c) H. Yan, T. H. LaBean, L. Feng, J. H. Reif, *Proc. Natl. Acad. Sci. U.S.A.* **2003**, *100*, 8103. d) T. H. LaBean, H. Yan, J. Kopatsch, F. Liu, E. Winfree, J. H. Reif, N. C. Seeman, *J. Am. Chem. Soc.* **2000**, *122*, 1848. e) C. Mao, W. Sun, N. C. Seeman, *J. Am. Chem. Soc.* **1999**, *121*, 5437. f) E. Winfree, F. Liu, L. A. Wenzler, N. C. Seeman, *Nature* **1998**, *394*, 539.

8 a) Y. Li, Y. D. Tseng, S. Y. Kwon, L. D'espaux, J. S. Bunch, P. L. Mceuen, D. Lou, *Nature Mater.* **2004**, *3*, 38. b) M. S. Shchepinov, K. U. Mir, J. K. Elder, M. D. Frank, M. S. Southern, *Nucleic Acids Res.* **1999**, *27*, 3035. c) M. Echeffler, A. Dorenbeck, S. Jordan M. Wustefeld, G. Kiedrowski, *Angew. Chem., Int. Ed.* **1999**, *38*, 3311. d) J. Wang, M. Jiang, *J. Am. Chem. Soc.* **1998**, *120*, 8281. e) J. Wang, G. Rivas, J. R. Fernandes, M. Jian, J. L. L. Paz, R. Waymire, T. W. Nielsen, R. C. Getts, *Electroanalysis* **1998**, *10*, 553. f) J. Shi, D. E. Bergstrom, *Angew. Chem., Int. Ed.* **1997**, *36*, 111. g) M. S. Shchepinov, I. A. Udalova, A. J. Bridgman, E. M. Southern, *Nucleic Acids Res.* **1997**, *25*, 4447.

9 a) R. Chhabra, J. Sharma, Y. Liu, H. Yan, *Nano Lett.* **2006**, *5*, 978. b) J. S. Shin, N. Pierce, *J. Am. Chem. Soc.* **2004**, *126*, 10834. c) P. Yin, H. Yan, X. G. Daniell, A. J. Turberfield, J. H. Reif, *Angew. Chem., Int. Ed.* **2004**, *43*, 4906. d) J. H. Reif, *Lect. Notes Comput. Sci.* **2003**, *2568*, 22.

10 a) J. Qi, X. Li, X. Yang, N. C. Seeman, *J. Am. Chem. Soc.* **1996**, *118*, 6121. b) X. Yang, A. V. Vologodskii, B. Liu, B. Kemper, N. C Seeman, *Biopolymers* **1998**, *45*, 69. c) P. Tosch, C. Walti, A. P. J. Middelberg, A. G. Davies, *Biomacromolecules* **2006**, *7*, 677.

11 a) T. Kuroda, Y. Sakurai, Y. Suzuki, A. O. Nakamura, M. Kuwahara, H. Ozaki, H. Sawai, *Chem. Asian J.* **2006**, *1*, 575. b) T. Horn, C. Chang, M. S. Urdea, *Nucleic Acids Res.* **1997**, *25*, 4835.

12 a) M. M. Rozenman, D. R. Liu, *ChemBioChem* **2006**, *7*, 253. b) X. Li, D. R. Liu, *Angew. Chem., Int. Ed.* **2004**, *43*, 4848.

13 a) Y. Yoshimura, D. Okamoto, M. Ogino, K. Fujimoto, *Org. Lett.* **2006**, *8*, 5049. b) M. Ogino, Y. Yoshimura, A. Nakazawa, I. Saito, K. Fujimoto, *Org. Lett.* **2005**, *7*, 2853. c) K. Fujimoto, N. Ogawa, M. Hayashi, S. Matsuda, I. Saito, *Tetrahedron Lett.* **2000**, *41*, 9437. d) K. Fujimoto, S. Matsuda, N. Takahashi, I. Saito, *J. Am. Chem. Soc.* **2000**, *122*, 5646.

14 a) M. Ogino, K. Fujimoto, *Angew. Chem., Int. Ed.* **2006**, *45*, 7223. b) S. Ogasawara, K. Fujimoto, *ChemBioChem* **2005**, *6*, 1756. c) K. Fujimoto, Y. Yoshimura, T. Ikemoto, A. Nakazawa, M. Hayashi, I. Saito, *Chem. Commun.* **2005**, 3177. d) K. Fujimoto, S. Matsuda, N. Ogawa, M. Hayashi, I. Saito, *Tetrahedron Lett.* **2000**, *41*, 6451.

15 a) S. Ogasawara, K. Fujimoto, *Angew. Chem., Int. Ed.* **2006**, *45*, 4512. b) Y. Yoshimura, Y. Noguchi, H. Sato, K. Fujimoto, *ChemBioChem* **2006**, *7*, 598.

16 M. Tagawa, K. Shohda, K. Fujimoto, A. Suyama, Proceedings of NanoBio-Tokyo, **2006**, p. 383.